Application of Gaussian Electrostatic Model (GEM) Distributed Multipoles in the AMOEBA Force Field

G. Andrés Cisneros*

Department of Chemistry, Wayne State University, Detroit, Michigan 48202, United States

ⓢ Supporting Information

ABSTRACT: We present the inclusion of distributed multipoles obtained from the Gaussian Electrostatic Model (GEM) into the AMOEBA force field. As a proof of principle, we have reparametrized water and alanine di-peptide. The GEM distributed multipoles (GEM−DM) have been obtained at the same levels of theory as those used for the original AMOEBA parametrization. The use of GEM allows the derivation of the distributed multipoles from the analytical fit to the molecular density or the numerical fit to the molecular electrostatic potential (mESP). In addition, GEM−DM are intrinsically finite of the highest order of the auxiliary basis used for the GEM fit. We also present the fitting of multipoles for the di-methyl imidazolium/ chloride (DMIM$^+$−Cl$^-$) ionic liquid pair. Results for intermolecular Coulomb for all test systems show very good agreement. MD simulations for a reparametrized AMOEBA water model with GEM−DM provide results on par with the original AMOEBA force field for a series of bulk properties including liquid density and enthalpy of vaporization. A package for the calculation of GEM Hermite coefficients and derived distributed multipoles using the numerical procedure is also presented and released under the GNU public license.

1. INTRODUCTION

The simulation of chemical and biochemical systems involves the use of classical empirical force fields.[1−5] These force fields use bonded and nonbonded contributions to calculate the energy of the systems. The latter include explicit Coulomb interactions. In general, these interactions are computed via atom centered point charges. However, this results in a loss of accuracy because of the loss of anisotropy as well as the failure to account for penetration effects.[6]

One way to improve the accuracy is to employ distributed multipoles.[6−8] Several force fields, including AMOEBA, SIBFA, EFP, and NEMO, that use distributed multipoles have been proposed.[9−12] The use of distributed multipoles introduces charge density anisotropy that is lost in isotropic point charge distributions and can significantly improve the treatment of electrostatics.[13−18] Despite this improvement, multipoles still suffer from charge penetration errors at close range.[6,19] This disadvantage may be addressed to an extent by the use of damping functions that correct the interaction energies at close intermolecular distances.[19−24]

Another possibility to avoid the anisotropy and charge penetration errors is to employ a continuous description of the molecular charge. Several methods that use either analytical or numerical forms of the charge density have been proposed.[25−30] We have recently introduced the Gaussian Electrostatic Model (GEM).[31,57,60] GEM uses density fitting (DF) methods[32−34] to expand the molecular density using Gaussian auxiliary basis sets (ABSs). The fitted densities, which may be obtained from any QM method that produces a relaxed one-electron density matrix, are employed to calculate each of the components of the intermolecular interaction separately. The GEM fragments are fitted to reproduce gas phase *ab initio* QM intermolecular interaction results from energy decomposition analysis (EDA).[35−49] The use of continuous functions

also provides a more accurate description of molecular properties compared to conventional point charges.[60]

The fitting of the molecular electronic densities is done to Hermite Gaussians. Two procedures may be employed, the conventional analytical variational Coulomb fitting or the numerical fit of molecular electrostatic potential.[50,51,60] The use of Hermite Gaussian functions for the ABS provides the added advantage that they lead to a natural definition of distributed multipole moments centered on the fitting sites. We term this distributed multipole decomposition GEM−DM.

In this contribution, we present the application of GEM− DM in the AMOEBA force field. We determine distributed multipoles for several systems including water, the alanine di-peptide, and the di-methyl imidazolium/chloride ion pair. Distributed multipoles for these systems are calculated with both the analytical and numerical procedures to compare the performance of each method. Additionally, two sets of ABSs are presented for the alanine di-peptide. The fitting of the GEM Hermites and derived GEM−DM are done with respect to reference quantum EDA data from basis set superposition (BSSE) corrected supermolecular calculations and restricted variational space (RVS) calculations.[41,52] All reference molecular densities for the chosen systems are calculated at the reference AMOEBA level (MP2/aug-cc-pVTZ or MP2/6-311+ +G(2d,2p)). A software package that implements the numerical fitting procedure is described and released under the GNU public license.

2. METHODS

In this section, we present the theory and computational details employed in the present study. In subsection 2.1, we provide a brief explanation of the analytical density fitting method and its implementation including the methods employed to control numerical instabilities. In subsection 2.2, we describe the numerical fit of the Hermite coefficients, followed by the procedure to calculate site multipoles from Hermite coefficients in subsection 2.3. Finally, subsection 2.4 presents the details of the calculations to obtain the molecular electronic densities and reference energy decomposition analysis.

2.1. Analytical Density Fitting. The use of ABSs for density fitting is a field of intense study. This method relies on the use of auxiliary basis functions, generally Gaussians, to expand the molecular electron density

$$\tilde{\rho}(r) = \sum_k x_k k(r) \tag{1}$$

The expansion coefficients x_k for the approximate density $\tilde{\rho}$ may be obtained by minimizing the self-energy of the error in the density according to some metric $\hat{O}$:[33,34,53,54]

$$E_{self} = \langle \rho(r) - \tilde{\rho}(r) | \hat{O} | \rho(r) - \tilde{\rho}(r) \rangle \tag{2}$$

The operator $\hat{O}$ can take several forms, including the overlap operator $\hat{O} = 1$, the Coulomb operator $\hat{O} = 1/r$, or the damped Coulomb operator $\hat{O} = \text{erfc}(\beta r)/r$.[55] The minimization of eq 2 with respect to the expansion coefficients x_k leads to a linear system of equations:

$$\frac{\partial E_{self}}{\partial x_l} = -\sum_{\mu,\nu} P_{\mu\nu} \left\langle \mu\nu | \hat{O} | l \right\rangle + \sum_k x_k \left\langle k | \hat{O} | l \right\rangle \tag{3}$$

where $P_{\mu\nu}$ is the density matrix. This equation may be used for the determination of the coefficients by setting

$$\mathbf{x} = \mathbf{G}^{-1}\mathbf{j} \tag{4}$$

where $\mathbf{j} = P_{\mu\nu}\langle \mu\nu | \hat{O} | l \rangle$ and $\mathbf{G} = \langle k | \hat{O} | l \rangle$.

In principle, $\mathbf{G}$ should be symmetric and positive definite. However in practice, this matrix is almost singular, and therefore the diagonalization to obtain its inverse must be done with care. We have explored both analytical and numerical methods to obtain $\mathbf{G}$ and its inverse.

In the analytical fitting procedure, we have implemented several methods for the diagonalization step. Initially, we employed singular value decomposition (SVD)[56] by setting the inverse of the eigenvalue to zero if it is below a certain cutoff. However, this method produces undesirable numerical instabilities (noise) when the number of basis functions starts to grow, as we and others have discussed previously.[57,58]

Subsequently, we opted to use the Tikhonov regularization formalism,[56] similar to the constrained density fitting algorithm proposed by Misquitta and Stone.[59] In this method, redundant basis set contributions are penalized by instead minimizing $E_{self} + \lambda \sum_k x_k^2$.[60] In addition, we implemented the damped Coulomb operator $\hat{O} = \text{erfc}(\beta r)/r$ proposed by Jung et al.[55] to attenuate the near singular behavior due to long-range interactions present in $\mathbf{G}$. In our studies, we observed that noise is still a problem, which was suggested to come from the attempt of the ABSs to fit the density at the nuclear cores.[57,60] An alternative fitting method to address this issue was explored as explained in the subsection below.

The use of Hermite Gaussians with angular moment greater than 0 requires the rotation of the fitting coefficients. This is due to the fact that higher order multipoles have directionality. To overcome this problem, we define a global molecular frame and a reference (local) site frame similar to AMOEBA. The use of Hermite Gaussians provides a straightforward solution to the transformation since they are defined by partial derivatives of a spherical Gaussian which can be taken either with respect to the local (reference) frame or with respect to the global coordinates.[60] Moreover, these frames are the same for the distributed multipoles and have been defined to be the same as the local frames used in AMOEBA for all the results below.

2.2. Numerical Fitting. The numerical instabilities arising from the analytical fitting due to the nuclear cores may be significantly decreased by instead performing the fitting using grids. The use of numerical grids allows the discarding of points at and near the core, thus effectively neglecting the core contributions. In this case, this is achieved by minimizing the following fitting function:

$$\chi^2 = \sum_i W(r_i)(y(\mathbf{r}_i) - \tilde{y}(\mathbf{r}_i, c_k))^2 \tag{5}$$

where $y(\mathbf{r}_i)$ denotes the *ab initio* molecular property of interest at point i and $\tilde{y}(\mathbf{r}_i, c_k)$ is the same property evaluated with the kth ABS element at the same point on the grid. Finally, $W(r)$ is the weighting function for the point on the grid, which can be defined in several ways.[61,62] The original weight function, e.g., for RESP fitting, neglects the points at and close to the core using a hard cutoff creating a discontinuity. Recently, Hu, Lu, and Yang have proposed a new weighting function that decays smoothly close to the cores and at long distances.[62]

$$W(r_i) = \exp[-\sigma(\log \rho_{promol}(\mathbf{r}) - \log \rho_{ref})^2] \tag{6}$$

Here, ρ_{promol} is a reference promolecular atomic density, and σ and ρ_{ref} are adjustable parameters. We have used a modified version of the Hu−Lu−Yang (HLY) weighting function previously.[51] It has been shown that the surface for σ and ρ_{ref} is pretty flat.[51,62] The main differences between the HLY weight and the present implementation are the reoptimization of the promolecular atomic electron densities at the MP2/aug-cc-pVQZ level and the values for σ and ρ_{ref}, which correspond to 0.42 and −7.0, respectively.

The minimization of eq 5 leads to a linear system of equations that can be expressed as $\mathbf{c} - c^0 = -H^{0,-1}g^0$. As was the case for the analytic DF in our previous study, we employ Tikhonov regularization for the inversion of the Hessian that arises for the linear-least-squares procedure. In this case, as above, we use a reference local frame for each fitting site in order to be able to transfer the calculated fitting coefficients.[60]

In our initial implementation of numerical fitting, we employed different molecular properties including electronic density, molecular electrostatic potential (mESP), and the three components of the electric field.[50] All of the properties were gridded on rectangular grids. Subsequently, we showed that the use of spherical molecular grids based on the scheme proposed by Becke[63] significantly reduces the number of fitting points.[51]

In the present implementation, we have employed only the mESP evaluated on spherical molecular grids obtained from code derived from ref 64. These expressions have been implemented by the author in a Fortran90 code, named GEM_fit, released under the GNU public license. The code allows the user to choose five pre-determined combinations of

radial and angular orders to generate extra-coarse, coarse, medium, fine, and extra-fine molecular grids based on the input coordinates. In addition, the user can choose to specify the number of radial and angular orders manually. The mESP is calculated automatically by evaluating the property at each point from a relaxed one-electron density matrix using either the cubegen utility from Gaussian 09 or by internal subroutines in the GEM_fit program.

2.3. Distributed Multipoles. In this subsection, we present the methodology to obtain Cartesian point multipoles from the Hermite coefficients obtained in the fitting procedure. Note that in the present contribution, as in our previous work, the highest order used for a Gaussian Hermite is 2. This ensures that the distributed multipoles obtained herein can be directly employed in the AMOEBA force field. However, higher order multipoles can be obtained if an ABS with higher angular momentum is used.

Briefly, we have expanded on the work of Challacombe et al., who have shown that Hermite Gaussians have a simple relation to elements of the Cartesian multipole tensor.[65] Once the Hermite coefficients have been determined, they may be employed to calculate point multipoles centered at the expansion sites. Thus, if hc_{tuv} represents the coefficient of a Hermite Gaussian of order Λ_{tuv}, then if this Hermite is normalized we have

$$hc_{000} \int \Lambda_0 \, dr = hc_{000} \tag{7}$$

This guarantees that higher order multipole integrals will integrate to integer numbers, for example, for the dipole integral in the x direction, $\mathbf{d}_x$:

$$hc_{100} \int\int\int x\Lambda_{100} \, dx \, dy \, dz$$
$$= hc_{100} \int x \frac{\partial}{\partial S_x} \Lambda_0 \, dx$$
$$= -hc_{100} \int x \frac{\partial}{\partial x} \Lambda_0 \, dx$$
$$= hc_{100} \tag{8}$$

For quadrupole and higher order integrals, the same relationships hold, although different cases need to be considered (see ref 60). In practice, following Stone's definition,[6] we have used traceless quadrupoles. Furthermore, the use of GEM−DM for multipolar force fields provides a straightforward way to determine the penetration error in the site−site Coulomb interaction energy due to the connection with the GEM Hermites. Thus, this connection provides a natural way to generate damping functions to lessen the penetration error.[21,22] This is currently under investigation.

A further advantage of this approach to distributed multipoles is that, unlike some conventional multipole expansions,[66,67] the (spherical) multipole expansion obtained from Hermite Gaussians in this way is intrinsically finite of order $t + u + v$ (i.e., the highest angular momentum in the ABS) as shown in ref 60, similar to the multipoles obtained by Volkov and Coppens.[28]

2.4. Computational Details. Relaxed one-electron molecular densities for the fitting procedures were obtained from *ab initio* calculations performed with Gaussian 09.[68] In the case of the water molecule, the density was obtained at the MP2(full)/aug-cc-pVTZ level using the AMOEBA equilibrium geometry.[69] For the alanine di-peptides and DMIM⁺−Cl⁻ ion pair, the QM

densities were obtained at the MP2(full)/6-311++G(2d,2p) and MP2(full)/6-311G(d,p) levels, respectively. All structures for the alanine di-peptides were optimized to match the test structures used by Ren and Ponder.[70] The structure of DMIM⁺ was optimized at the same level of theory as above. Generalized distributed multipole analysis (GDMA) multipoles for the reference calculations (except for water) were calculated using the same formatted checkpoint files with the GDMA program[71] following the same guidelines for GDMA multipoles for AMOEBA as detailed in ref 72.

Reference values for all of the systems were calculated at the corresponding levels of theory and basis sets with supermolecular BSSE corrected calculations. We have also written a program that allows the calculation of intermolecular Coulomb interaction from frozen *ab initio* relaxed densities. This program was employed to obtain the Coulomb energy surfaces. Intermolecular polarization interactions were calculated with RVS at the HF level with the same basis sets as above using the GAMESS program.[73]

The density fit was done with the A1 ABS for water and the alanine di-peptides. In the case of DMIM⁺, we have considered two different ABSs corresponding to the A1 and A2 Coulomb fitting ABS from the DGauss DFT program.[74,75] In the case of the water molecule, only the numerical fitting procedure has been considered. For the other two systems both numerical and analytical fits have been explored. The calculated density matrices were used as input for the program described in the Methods section to obtain the local Hermite coefficients and distributed multipoles for the corresponding ABSs. In the case of both the analytical and numerical fits, there is one parameter that can be used to control the noise in the fit. This corresponds to the λ parameter in the Tikhonov regularization.

In all cases, the λ parameter has been optimized so that the error in the intermolecular Coulomb interactions from the GEM Hermites is minimized with respect to *ab initio* reference calculations for a series of hydrogen bonded dimers (see Figure 1). For the water molecule, the canonical water dimer at
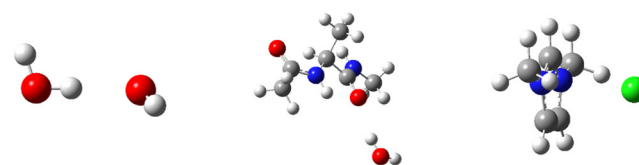

Figure 1. Dimers used for the calculation of intermolecular Coulomb interactions for reference calculations and fitting optimization.

different distances was employed. In the case of the alanine dipeptide a di-Ala/water dimer was used at three to five different distances for each of the four conformers fitted. In the case of the DMIM⁺−Cl⁻ dimer, the intermolecular Coulomb interaction for this dimer at different distances was employed. The optimized values for the λ's are reported in the Supporting Information.

For all of the numerical fit,s only coarse grids were employed, resulting in fitting on 29 080, 201 000 (approx), 147 251, and 9664 grid points for water, di-alanine, DMIM⁺, and Cl⁻, respectively. All Becke grids were generated automatically using a modified version of the HPAM program[64] that has been included in the GEM_fit package.

Once the Hermite coefficients and derived distributed multipoles were determined, they were transformed to TINKER format by a modified utility program (poledit) in

TINKER and to AMBER format. The definition of the local frames for GEM was used also in the AMOEBA local frames. The calculation of the intramolecular induction and reoptimization of the multipoles was performed with the "potential" program in the TINKER software suite. In this case, the reoptimization of the multipoles is done by calculating the electrostatic potential (at the same or higher level of theory) on a rectangular grid and refitting the distributed multipoles (keeping the monopoles fixed). This procedure is described in the Supporting Information of ref 72. All intermolecular interactions involving multipoles were obtained with TINKER,[76] and the molecular dynamics simulations for water were calculated with the AMOEBA implementation in AMBER11.[1] The MD simulations were carried out on a cubic box containing 216 AMOEBA water molecules at constant pressure ($P = 1$ bar) and temperature (298 K) for 1.5 ns with a 1 fs time step. Particle mesh Ewald was used for long-range electrostatic interactions with a direct space and van der Waals cutoff of 7.5 Å.[77−79] The induced dipoles were converged to 0.01 D RMSD, and the equations of motion were integrated with a modified Beeman algorithm using a Berendsen thermostat and barostat.[80]

3. RESULTS AND DISCUSSION

In this section, we present and discuss the results for the three test systems. In subsection 3.1, the results for the numerical fitting of GEM distributed multipoles for water, optimization of van der Waals parameters and Tholè damping function, and results for intermolecular interactions and MD simulations are discussed. Subsection 3.2 describes the analytical and numerical fitting of the distributed multipoles for the alanine di-peptide in five different conformations and the comparison of the mESP calculated with the multipoles to the mESP obtained from *ab initio* calculations on a mesh of points around the molecules. Subsection 3.3 deals with the results for the fitting of GEM−GM for the DMIM⁺−Cl⁻ ion pair along with results for intermolecular Coulomb interactions using two different ABSs.

3.1. Water. For the water simulation, only Hermite coefficients and multipoles with the A1 ABS from the numerical fitting procedure have been calculated. This is due to the fact that we have previously shown that the use of numerical fitting for the determination of Hermite coefficients for water leads to a significant reduction in the number of primitive Gaussians required for accurate results (41 vs 110 primitives).[50] The combination of A1 ABS and numerical fit gives very accurate results for water. The average and maximum errors for the intermolecular Coulomb interaction for 10 water dimers is 0.06 and 0.16 kcal/mol, respectively, well below k_BT at room temperature.[50]

The A1 ABS includes only *s*-type functions on H; therefore, the final distributed multipoles for the current water model involve moments up to quadrupoles on oxygen and only monopoles on the H atoms. The magnitude of the $l = 0$ moments for the present model correspond to −0.925 for O and 0.4625 for H. These values are significantly higher than the charges obtained with a GDMA of −0.5197 and 0.2598 for O and H, respectively. Tables S1 and S2 in the Supporting Information show all the atomic multipoles (up to quadrupole) for GEM−DM and the original AMOEBA parametrization for comparison. Interestingly, the present charges agree well with those reported for the density fragment approach (−0.942 for O and 0.471 for H), which also uses the HLY weight function to calculate ESP fitted charges.[81] Moreover, this is a direct

result of the fact that atom-based distributed multipoles are highly underdetermined, and different methods giving very different distributed multipoles provide accurate results for molecular properties (i.e., mESP) and intermolecular Coulomb interactions (see below).

Figure 2 shows the total intermolecular interaction and each nonbonded component (Coulomb, polarization and van der
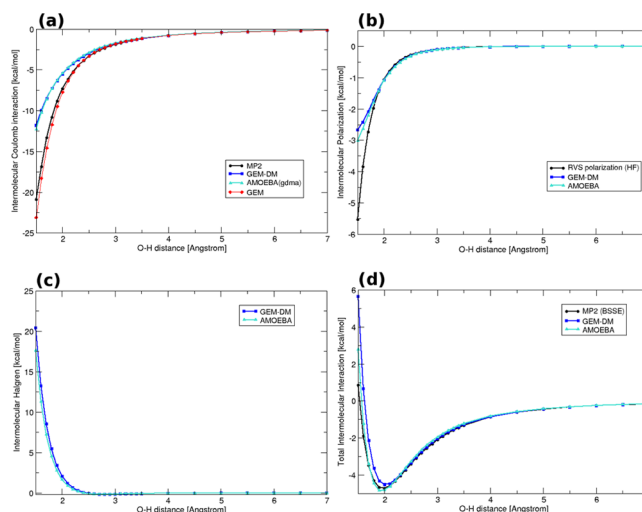

Figure 2. Comparison of interaction energies for the canonical water dimer calculated with AMOEBA, AMOEBA/GEM−DM, and *ab initio*. (a) Coulomb, (b) polarization (reference from RVS), (c) van der Waals, (d) total.

Waals) as per the AMOEBA model. The Coulomb interactions (Figure 2a) calculated with GEM−DM are on average 0.1 kcal/mol more negative (closer to the *ab initio*) than the GDMA multipoles in the range of 2.0−3.5 Å. Errors in Coulomb interaction from both multipolar decompositions around 2.5 Å between the O and H are around 0.5 kcal/mol with respect to *ab initio*, i.e., close to k_BT. This error increases dramatically as the distance is decreased below 2.5 Å, demonstrating the impact of the penetration error. In comparison, the GEM Hermites are shown to follow the reference *ab initio* curve even at close distances. Indeed, the errors around hydrogen bonding distances for GEM are below 10% (out of approximately 10 kcal/mol) compared to over 30% for the distributed multipoles (see Figure S14 in the Supporting Information). This error is reduced as the distance increases and tends to 0 at long range.

In the case of the polarization interaction, the Tholé exponent for the calculation using GEM−DM has been reduced to 0.35 (from the original 0.39). We have previously used a modified Tholé parameter for the investigation of divalent cations in water.[82] The reduction in the damping exponent results in curves that are indistinguishable between the original AMOEBA polarization and the polarization calculated with the GEM distributed multipoles (see Figure 2b). Both the GEM−DM and AMOEBA polarization contributions are in good agreement with the reference RVS calculation. As mentioned above, RVS is only available at the Hartree−Fock level and does not include perturbation corrections. Thus, the curve only presents an approximation to the polarization contribution from the MP2 molecular densities.

For the van der Waals term, the atomic radii and well depths for the buffered Halgren function have been modified from the

original AMOEBA parameters to reproduce the total intermolecular interaction of the dimer and the liquid density. As can be seen from Figure 2c, the AMOEBA and GEM−DM curves overlap for almost the entire distance range considered. The combination of the nonbonded terms results in a total intermolecular interaction curve that closely matches the reference MP2 (BSSE corrected) until the minimum (see Figure 2d). For distances closer than 1.9 Å, the GEM−DM based model shows a steeper increase than the AMOEBA curve. This is likely due to the larger magnitude of the charges, which result in larger Coulomb repulsion at short range.

On the basis of the parameters calculated above, an NPT simulation on a box containing 216 waters was performed. The average density for the liquid from these calculations is 1.0096 g cm^{-1}, which is slightly higher than the result obtained with the original AMOEBA parameters of 1.0004 g cm^{-1}. Our calculated value is 1.28% higher than the experimental density of 0.9970 g cm^{-1}.

The heat of vaporization can be calculated from the difference in potential energies between the liquid and gas phases, assuming that the water vapor behaves ideally:

$$\Delta H_V = -\Delta E + \Delta PV = E_{liq} + E_{gas} + RT \qquad (9)$$

The average potential energy of the liquid from the NPT simulation is −8.98 kcal/mol. The potential energy of the gas determined from stochastic dynamics of a monomer at room temperature using a time step of 0.1 fs is E_{gas} = 0.90 kcal/mol. Therefore, the calculated heat of vaporization at 298 K is 10.47 kcal/mol compared to the value calculated with AMOEBA of 10.48 kcal/mol, and both are close to the experimental value of 10.51 kcal/mol.

Radial distribution functions (rdfs) have been determined to characterize the structure of liquid water and compared to those calculated with the original AMOEBA model and experimental curves from neutron scattering data.[83] Figure 3 shows the rdfs for O−O, O−H, and H−H for the GEM−DM based model, AMOEBA, and experimental results. As can be seen, the structure for both models is very similar. The peaks and valleys calculated with both methods agree overall. The only differences are in the O−O rdf where the heights of the first and second valleys as well as the height of the second peak are approximately 6% smaller for the GEM−DM model. The second difference is in the position of the first peak on the O−H rdf, which is shifted by 0.1 Å to the right in the GEM−DM model. This last feature could be due to the fact that the minimum on the PES of the canonical water dimer for the MP2(full)/aug-cc-pVTZ reference is centered at 2.0 Å. The GEM−DM model matches this as the minimum, whereas the AMOEBA model shows a flatter minimum with two almost isoenergetic points at 2.0 and 1.9 Å (see Figure 2d).

3.2. Alanine Dipeptide. In order to allow the transferability of the site multipoles for different conformations, the AMOEBA force field explicitly includes intramolecular polarization.[70] This is achieved by considering that the distributed multipoles on each site include "permanent" and "induced" components. By removing the "induced" moments from the calculated distributed multipoles, we are left with only the "permanent" term. The "permanent" multipoles along with the intramolecular polarization can then be used to calculate the full multipoles for any arbitrary conformation.[70]

Ren and Ponder presented an analytical formula to perform this decomposition based on polarization groups. In this method, the permanent atomic multipoles polarize between
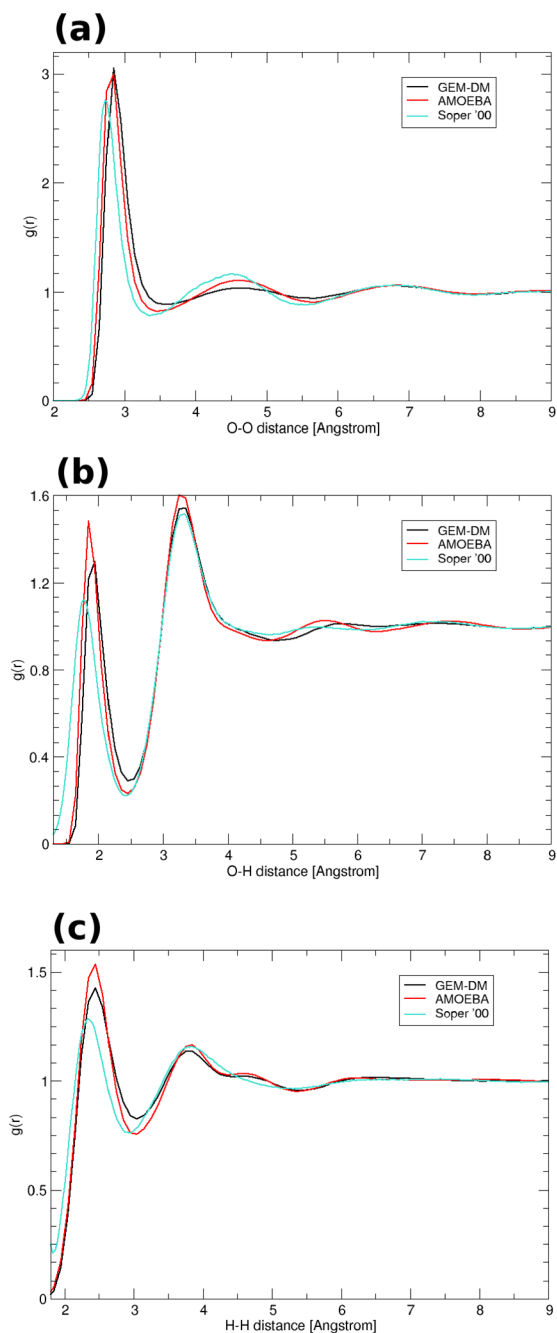

Figure 3. Comparison of radial distribution functions (rdfs) calculated with AMOEBA and AMOEBA/GEM−DM. (a) O−O rdf, (b) O−H rdf, (c) H−H rdf. Soper '00 denotes the neutron scattering derived experimental curve from ref 83.

groups only; i.e., there is only intergroup polarization but not intragroup polarization. This procedure was tested on different conformations of the alanine di-peptide by fitting GDMA multipoles for four different conformations, performing the multipole decomposition and employing the "permanent" multipoles and intramolecular polarization for a fifth conformation. The calculated multipoles were used to calculate the mESP on a grid of points and calculate the deviation with respect to ab initio.[70]

Recently, Ren et al. have reported a procedure for flexible molecules that involves the determination of distributed multipoles for several conformations of the same molecule

Table 1. RRMSD and RMSD Comparisons of ESPs for Five Alanine Dipeptide Conformers Computed by *ab Initio* (MP2(full)/6-311++G(2d,2p)), GDMA Multipoles, and GEM−DM Using Analytical (ANA) or Numerical (NUM) Fits[a]

	α_L		C5		C7a		C7e		α'	
	ANA	NUM	ANA	NUM	ANA	NUM	ANA	NUM	ANA	NUM
GEM−DM	0.46(0.37)	0.13(0.10)	1.06(0.43)	0.22(0.09)	1.11(0.46)	0.18(0.07)	0.45(0.09)	0.93(0.31)	7.38(4.32)[d]	12.50(9.34)[d]
GEM−DM +ind[b]	2.07(1.71)	9.72(24.66)	5.64(2.86)	15.89(24.69)	4.43(2.27)	12.41(9.79)	5.65(2.32)	19.26(22.90)	10.85(5.40)[e]	15.93(22.81)[e]
GEM−DM +ind OPT[c]	0.64(0.50)	0.71(0.56)	0.96(0.39)	1.91(0.79)	1.21(0.51)	0.90(0.38)	1.55(0.53)	2.91(1.00)	0.88(0.59)[f]	1.70(1.08)[f]
GDMA	1.65(1.32)		2.21(0.92)		4.24(1.86)		3.24(1.17)		n/c	

[a]RRMSD values are reported as percentages. RMSD values listed in parentheses are in kcal/mol. [b]GEM−DM with AMOEBA induced multipoles (group 1−2 induction[70]). [c]GEM−DM with AMOEBA induced multipoles (group 1−2 induction) after reoptimization as in ref 72. [d]Average GEM−DM (see text). [e]Merged GEM−DM (see text). [f]Merged GEM−DM after reoptimization.

followed by the calculation of mESP points and comparison to *ab initio* and a final reoptimization of the multipoles to reproduce the mESP with respect to reference *ab initio* values.[72]

To test the transferability between different conformers for GEM−DM, we have performed similar calculations for the alanine di-peptide. To this end, we calculated GEM−DM for four conformers: α_L, C5, C7a, and C7e. In addition, GEM−DM permanent multipoles plus explicit AMOEBA intramolecular polarization (GEM−DM+ind), as well as GEM−DM+ind following the reoptimization procedure (GEM−D+ind OPT), have been determined for each conformer. Finally, two sets of "merged" multipoles have been obtained, one that includes all four fitted conformers and the intramolecular polarization, and this same set was subjected to the reoptimization procedure.

Following Ren and Ponder, these multipoles were tested by comparing the mESP calculated with the multipoles against *ab initio* results calculated at the same level used to determine the multipoles (MP2(full)/6-311++G(2d,2p)). The comparisons were done by means of root-mean-square deviations (RMSD) and relative RMSD (RRMSD). The mESP from both multipoles and *ab initio* were calculated on an average of 12 000 points around the each molecule. The RMSD and RRMSD results are presented in Table 1. As can be seen, the mESP is very well reproduced by the GEM multipoles independent of the fitting procedure employed for the multipoles corresponding to each conformer (GEM−DM). In fact, the deviations obtained from GEM−DM are at least two times smaller than those calculated with GDMA multipoles.

In order to demonstrate the nontransferability of the multipoles, we calculated average multipoles based on the four conformers and used these to calculate the mESP for a fifth conformer, α'. The calculated deviations from the average multipoles are at least seven times larger than for the conformers where the multipoles were calculated explicitly.

The use of the explicit AMOEBA intramolecular polarization results in an increase in the RRMSD for the analytically fitted multipoles. This is similar to what was reported by Ren and Ponder.[70] The use of intramolecular polarization for the numerically fitted multipoles gives significantly larger deviations. Once the GEM−DM+ind sets for each conformer were obtained, they were subjected to the reoptimization procedure.[72] The reoptimized GEM−DM shows a significant improvement for all conformers, especially for the numerically fit GEM−DM. The difference in transferability for the analytically vs numerically obtained multipoles might be due to the fact that the analytical GEM−DMs are obtained from Hermites that reproduce the molecular density. Conversely, the numerical GEM−DMs are optimized to reproduce the mESP

of a particular conformer and involve the neglect of points close to the core.

The final set of multipoles involves the use of all four fitted sets to determine a new combined set which we denote merged GEM−DM. The merged multipoles plus intermolecular polarization have been tested on the α' conformer, giving relatively high deviations from the reference. However, once the merged multipoles are reoptimized the results for the conformer not in the fitting set shows a remarkable improvement as can be seen in Table 1.

These results show that the multipoles obtained from GEM are suitable for the AMOEBA procedure and provide a viable procedure for the calculation of transferable AMOEBA multipoles. As mentioned above, the fact that the GEM−DM multipoles are as transferable as the original GDMA multipoles used in AMOEBA is another example of the underdetermined nature of the distributed multipoles. It should be noted that, as was the case with water, only the A1 ABS has been employed for the fit of the alanine dipeptide. Therefore, the GEM multipoles for all the hydrogen atoms include only monopole terms.

3.3. Dimethyl Imidazolium−Chloride Ion Pair. For the DMIM$^+$−Cl$^-$ ion pair, two sets of multipoles have been determined. The first was obtained from the Hermite coefficients using the A1 ABS and the second from the A2 ABS. Figure 4 shows the intermolecular electrostatic interaction for the DMIM$^+$−Cl$^-$ ion pair for the reference MP2, GEM Hermite (A1 and A2), GEM−DM (from A1 and A2), and GDMA. As expected, the Coulomb interaction calculated with the GEM Hermites for both ABSs using either the numerical or analytical fit show very good agreement at long and medium range and start to deviate around 3.2 Å separation. In comparison, the intermolecular Coulomb interactions calculated with the distributed multipoles shows larger deviations at this and longer ranges due to the penetration error (see Figure S15 in the Supporting Information), similar to the case of the water dimer (subsection 3.1).

Intermolecular Coulomb interactions calculated with GEM−DM obtained with the A2 ABS using both fitting procedures agree at long range and start to show deviations around 3.5 Å and below. The GDMA multipoles show similar performance to the GEM−DM (A2) multipoles, although the GDMA multipoles exhibit a constant overestimation of the intermolecular interaction at long range. The GDMA multipoles show almost a negligible improvement after reoptimization of the multipoles with the AMOEBA ESP refitting procedure. In the case of the GEM−DM(A2) multipoles, the intermolecular interactions are seen to show a decrease in accuracy for both
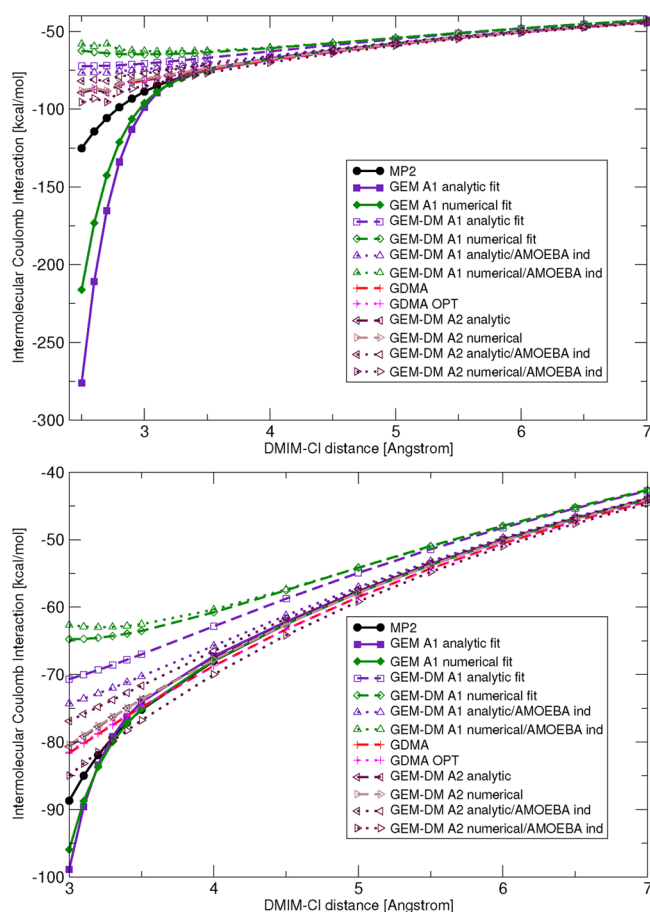
Figure 4. Coulomb intermolecular interaction for DMIM$^+$−Cl$^-$ calculated with different multipoles, GEM Hermites, and reference MP2 densities. Bottom shows close up from 3 to 7 Å.

the numerical and analytically fit multipoles after reoptimization.

In the case of the GEM−DM with the A1 ABS, both with the numerical and analytical fit, the intermolecular interactions show a consistent underestimation for both sets. This underestimation is increased in the case of the numerical fit. The GEM−DM (A1) multipoles show a slight improvement after they have been subjected to the AMOEBA reoptimization procedure. However, the reoptimized GEM−DM multipoles including the AMOEBA intramolecular polarization still show significant errors with respect to the *ab initio* reference.

As mentioned above, the A1 ABS only includes *s* type functions on H atoms. This results in GEM−DMs with only monopole terms on the hydrogens. The reoptimization and inclusion of intramolecular polarization results in the inclusion of dipole terms on the H atoms. However, this is not sufficient to give an accurate description of the ion pair Coulomb interaction. In contrast, the A2 ABS includes p and d type functions on H, giving rise to dipole and quadrupole terms for the GEM−DM on these atoms. This results in good agreement of the GEM−DM (A2) surfaces with the *ab initio* reference as discussed above.

The inaccuracies are due to the poor description of the electrostatic potential, in particular around the H atoms and in the center of the ring (see Supporting Information). Indeed, the mESP calculated with GEM−DM from the A1 basis (in both fitting methods) shows less anisotropy compared to the GEM−DM from A2. Moreover, the differences in mESP with

respect to *ab initio* are larger for the A1 multipoles than for the ones obtained for the A2 ABS. In addition to the electrostatics, van der Waals and bonded parameters for this ion pair are currently being developed for AMOEBA.

4. CONCLUSIONS

Distributed multipoles based on the Gaussian Electrostatic Model (GEM−DM) have been applied in the AMOEBA force field. Two sets of multipoles have been determined on the basis of either analytical or numerical fits of the Gaussian Hermite coefficients. The systems considered to test the applicability of the distributed multipoles include water, alanine dipeptide, and the dimethylimidazolium−chloride ion pair. Energy components and bulk properties from MD simulations for water give results that are in agreement with the original AMOEBA parameters. Transferability of the GEM multipoles for different molecular conformations was shown by the calculation of mESP around different conformers of the alanine dipeptide. Direct GEM−DM and optimized GEM−DM including AMOEBA intramolecular polarization for the different conformers give relative RMS deviations below 2% in almost all the cases. For both the water and dialanine systems, only A1 ABSs were considered, where all H atoms only result in monopolar terms. For the ionic liquid ion pair (DMIM$^+$−Cl$^-$), both A1 and A2 ABSs were utilized to derive GEM distributed multipoles. It is observed that for highly charged systems it is necessary to include higher order multipoles on the H atoms. GEM−DM provides an alternative to conventional methods for determination of distributed moments with the attractive features that the multipoles from GEM−DM are intrinsically finite, the multipoles derived from densities obtained with diffuse functions are numerically stable, and the resulting multipoles are easily transferable between conformations. A software package, GEM_fit, is released under GPL that implements the numerical fitting procedure for GEM Hermites and associated distributed multipoles.

■ ASSOCIATED CONTENT

ⓢ Supporting Information

Optimal fitting parameters for all molecules tested in this study, optimized multipoles and sample coordinates in TINKER format for all three test systems and Halgren parameters for water with GEM−DM, differences in mESP for A2 Hermites, A2 analytical GEM−DM, A2 numerical GEM−DM, A1 analytical GEM−DM and A1 numerical GEM−DM with respect to *ab initio*, error in intermolecular Coulomb interaction for the water dimer, and error in intermolecular Coulomb interaction for the IL ion pair. This material is available free of charge via the Internet at http://pubs.acs.org.

■ AUTHOR INFORMATION

Corresponding Author

*E-mail: andres@chem.wayne.edu.

Notes

The authors declare no competing financial interest.

■ ACKNOWLEDGMENTS

■ REFERENCES

(1) Case, D. A.; Cheatham, T. E., III; Darden, T. A.; Gohlke, H.; Luo, R.; Merz, K. M., Jr.; Onufirev, A.; Simmerling, C.; Wang, B.; Woods, R. J. *J. Comput. Chem.* **2005**, *26*, 1668−1688.

(2) Jorgensen, W. L.; Tirado-Rives, J. *J. Comput. Chem.* **2005**, *26*, 1669−1700.

(3) van der Spoel, D.; Lindahl, E.; Hess, B.; Groenhoff, G.; Mark, A. E.; Berensen, H. J. C. *J. Comput. Chem.* **2005**, *26*, 1701−1718.

(4) Christen, M.; Hünenberger, P. H.; Bakowies, D.; Baron, R.; Brúgl, R.; Geerke, D. P.; Heinz, T. N.; Kastenholz, M. A.; Kräutler, V.; Oostenbrink, C.; Peter, C.; Trzesniak, D.; van Gunsteren, W. F. *J. Comput. Chem.* **2005**, *26*, 1719−1751.

(5) MacKerrell, A. D., Jr.; Brooks, B.; Brooks, C. L., III,; Roux, N. B.; Won, Y.; Karplus, M. CHARMM: The energy function and its parametrization with an overview of the program. In *Encyclopedia of Computational Chemistry*; John Wiley & Sons Ltd.: New York, 1998; pp 271−277.

(6) Stone, A. J. *The Theory of Intermolecular Forces*; Oxford University Press: Oxford, U.K., 2000.

(7) Stone, A. J. *Chem. Phys. Lett.* **1981**, *83*, 233−239.

(8) Vigné-Maeder, F.; Claverie, P. *J. Chem. Phys.* **1988**, *88*, 4934−4948.

(9) Hermida-Ramón, J. M.; Brdarski, S.; Karlström, G.; Berg, U. *J. Comput. Chem.* **2003**, *24*, 161−176.

(10) Gresh, N.; Cisneros, G. A.; Darden, T. A.; Piquemal, J.-P. *J. Chem. Theory Comput.* **2007**, *3*, 1960−1986.

(11) Ponder, J. W.; Wu, C.; Ren, P.; Pande, V. S.; Chodera, J. D.; Schnieders, M. J.; Haque, I.; Mobley, D. L.; Lambrecht, D. S.; DiStasio, R. A., Jr.; Head-Gordon, M.; Clark, G. N. I.; Johnson, M. E.; Head-Gordon, T. *J. Phys. Chem. B* **2010**, *114*, 2549−2564.

(12) Day, P. N.; Jensen, J. H.; Gordon, M. S.; Webb, S. P.; Stevens, W. J.; Krauss, M.; Garmer, D.; Basch, H.; Cohen, D. *J. Chem. Phys.* **1996**, *105*, 1968−1986.

(13) Stone, A. J. *The Theory of Intermolecular Forces*; Clarendon Press: Oxford, U. K., 1996.

(14) Price, S. Toward more accurate Model Intermolecular Potentials for Organic Molecules. In *Reviews in Computational Chemistry*; Lipkowitz, K., Boyd, D. B., Eds.; VCH Publishers: New York, 1999; Vol. *14*, pp 225−289.

(15) Popelier, P. *Atoms in Molecules: An Introduction*; Prentice Hall: Harlow, England, 2000.

(16) Kosov, D. S.; Popelier, P. L. A. *J. Phys. Chem. A* **2000**, *104*, 7339−7345.

(17) Popelier, P. L. A.; Joubert, L.; Kosov, D. S. *J. Phys. Chem. A* **2001**, *105*, 8254−8261.

(18) Popelier, P. L. A.; Kosov, D. S. *J. Chem. Phys.* **2001**, *114*, 6539−6547.

(19) Freitag, M. A.; Gordon, M. S.; Jensen, J. H.; Stevens, W. J. *J. Chem. Phys.* **2000**, *112*, 7300−7306.

(20) Kairys, V.; Jensen, J. H. *Chem. Phys. Lett.* **1999**, *315*, 140−144.

(21) Piquemal, J.-P.; Gresh, N.; Giessner-Prettre, C. *J. Phys. Chem. A* **2003**, *107*, 10353−10359.

(22) Cisneros, G. A.; Tholander, S. N.-I.; Parisel, O.; Darden, T. A.; Elking, D.; Perera, L.; Piquemal, J.-P. *Int. J. Quantum Chem.* **2008**, *108*, 1905−1912.

(23) Wang, B.; Truhlar, D. G. *J. Chem. Theory Comput.* **2010**, *6*, 3330−3342.

(24) Stone, A. J. *J. Phys. Chem. A* **2011**, *115*, 7017−7027.

(25) Wheatley, R. *Mol. Phys.* **2011**, *7*, 761−777.

(26) Gavezzotti, A. *J. Phys. Chem. B* **2002**, *106*, 4145−4154.

(27) Eckhardt, C. J.; Gavezzotti, A. *J. Phys. Chem. B* **2007**, *111*, 3430−3437.

(28) Volkov, A.; Coppens, P. *J. Comput. Chem.* **2004**, *25*, 921−934.

(29) Coppens, P.; Volkov, A. *Acta Crystallogr., Sect. A* **2004**, *60*, 357−364.

(30) Paricaud, P.; Predota, M.; Chialvo, A. A.; Cummings, P. T. *J. Chem. Phys.* **2005**, *122*, 244511.

(31) Piquemal, J. P.; Cisneros, G. A.; Reinhardt, P.; Gresh, N.; Darden, T. A. *J. Chem. Phys.* **2006**, *124*, 104101.

(32) Boys, S. F.; Shavit, I. *A Fundamental Calculation of the Energy Surface for the System of Three Hydrogen Atoms*; AD212985, NTIS: Springfield, VA, 1959.

(33) Dunlap, B. I.; Connolly, J. W. D.; Sabin, J. R. *J. Chem. Phys.* **1979**, *71*, 4993−4999.

(34) Köster, A. M.; Calaminici, P.; Gómez, Z.; Reveles, U. Density functional theory calculation of transition metal clusters. In *Reviews of Modern Quantum Chemistry, A Celebration of the Contribution of Robert G. Parr*; World Scientific: Singapore, 2002; pp 1439−1475.

(35) Eisenschitz, R.; London, F. *Z. Phys.* **1930**, *60*, 491−527.

(36) Hirshfelder, J. O. *Chem. Phys. Lett.* **1967**, *1*, 325−329.

(37) Hirshfelder, J. O. *Chem. Phys. Lett.* **1967**, *1*, 363−368.

(38) Murrel, J. N.; Shaw, G. *J. Chem. Phys.* **1967**, *46*, 1768−1772.

(39) Kitaura, K.; Morokuma, K. *Int. J. Quantum Chem.* **1976**, *10*, 325−340.

(40) Bagus, P. S.; Hermann, K.; Bauschlicher, C. W., Jr. *J. Chem. Phys.* **1984**, *80*, 4378−4386.

(41) Stevens, W. J.; Fink, W. H. *Chem. Phys. Lett.* **1987**, *139*, 15−22.

(42) Jeziorski, B.; Moszynski, R.; Szalewicz, K. *Chem. Rev.* **1994**, *94*, 1887−1930.

(43) Glendening, E. D.; Streitwieser, A. *J. Chem. Phys.* **1994**, *100*, 2900−2909.

(44) Glendening, E. D. *J. Am. Chem. Soc.* **1994**, *118*, 2473−2482.

(45) Mo, Y.; Gao, J.; Peyerimhoff, S. D. *J. Chem. Phys.* **2000**, *112*, 5530−5538.

(46) Heßelmann, A.; Jansen, G.; Schütz, M. *J. Chem. Phys.* **2005**, *122*, 14103−14120.

(47) Piquemal, J.-P.; Marquez, A.; Parisel, O.; Giessner-Prettre, C. *J. Comput. Chem.* **2005**, *26*, 1052−1062.

(48) Khaliullin, R. Z.; Head-Gordon, M.; Bell, A. T. *J. Chem. Phys.* **2006**, *124*, 204105.

(49) Lu, Z.; Zhou, N.; Wu, Q.; Zhang, Y. *J. Chem. Theory Comput.* **2011**, *7*, 4038−4049.

(50) Cisneros, G. A.; Elking, D. M.; Piquemal, J.-P.; Darden, T. A. *J. Phys. Chem. A* **2007**, *111*, 12049−12056.

(51) Elking, D. M.; Cisneros, G. A.; Piquemal, J.-P.; Darden, T. A.; Pedersen, L. G. *J. Chem. Theory Comput.* **2010**, *6*, 190−202.

(52) Boys, S.; Bernardi, F. *Mol. Phys.* **1970**, *19*, 553−566.

(53) Eichkorn, K.; Treutler, O.; Öhm, H.; Häser, M.; Ahlrichs, R. *Chem. Phys. Lett.* **1995**, *240*, 283−290.

(54) Köster, A. M. *J. Chem. Phys.* **1996**, *104*, 4114−4124.

(55) Jung, Y.; Sodt, A.; Gill, P. M. W.; Head-Gordon, M. *Proc. Natl. Acad. Sci. U. S. A.* **2005**, *102*, 6692−6697.

(56) Press, W. H.; Teukolsky, S. A.; Vetterling, W. T.; Flannery, B. P. *Numerical Recipes in Fortran77; the Art of Scientific Computing*, 2nd ed.; Cambridge University Press: New York, 1992; pp 799−803.

(57) Cisneros, G. A.; Piquemal, J.-P.; Darden, T. A. *J. Chem. Phys.* **2005**, *123*, 044109.

(58) Podeszwa, R.; Bukowski, R.; Szalewicz, K. *J. Chem. Theory Comput.* **2006**, *2*, 400−412.

(59) Misquitta, A. J.; Stone, A. J. *J. Chem. Phys.* **2006**, *124*, 024111.

(60) Cisneros, G. A.; Piquemal, J.-P.; Darden, T. A. *J. Chem. Phys.* **2006**, *125*, 184101.

(61) Bayly, C. I.; Cieplak, P.; Cornell, W. D.; Kollman, P. A. *J. Phys. Chem.* **1993**, *97*, 10269−10280.

(62) Hu, H.; Lu, Z.; Yang, W. *J. Chem. Theory Comput.* **2007**, *3*, 1004−1013.

(63) Becke, A. D. *J. Chem. Phys.* **1988**, *88*, 2547−2553.

(64) Elking, D. M.; Perera, L.; Pedersen, L. G. *Comput. Phys. Commun.* **2012**, *183*, 390−397.

(65) Challacombe, M.; Schwgler, E.; Almlöf, J. Modern developments in Hartree−Fock theory: Fast methods for computing the Coulomb matrix. In *Computational Chemistry: Review of Current Trends*; World Scientific Inc.: Singapore, 1996; pp 53−107.

(66) Stone, A. J. *J. Chem. Theory Comput.* **2005**, *1*, 1128−1132.

(67) Popelier, P. L. A.; Joubert, L.; Kosov, D. S. *J. Phys. Chem. A* **2001**, *105*, 8524−8261.

(68) Frisch, M. J.; Trucks, G. W.; Schlegel, H. B.; Scuseria, G. E.; Robb, M. A.; Cheeseman, J. R.; Scalmani, G.; Barone, V.; Mennucci,

B.; Petersson, G. A.; Nakatsuji, H.; Caricato, M.; Li, X.; Hratchian, H. P.; Izmaylov, A. F.; Bloino, J.; Zheng, G.; Sonnenberg, J. L.; Hada, M.; Ehara, M.; Toyota, K.; Fukuda, R.; Hasegawa, J.; Ishida, M.; Nakajima, T.; Honda, Y.; Kitao, O.; Nakai, H.; Vreven, T.; Montgomery, J. A., Jr.; Peralta, J. E.; Ogliaro, F.; Bearpark, M.; Heyd, J. J.; Brothers, E.; Kudin, K. N.; Staroverov, V. N.; Kobayashi, R.; Normand, J.; Raghavachari, K.; Rendell, A.; Burant, J. C.; Iyengar, S. S.; Tomasi, J.; Cossi, M.; Rega, N.; Millam, J. M.; Klene, M.; Knox, J. E.; Cross, J. B.; Bakken, V.; Adamo, C.; Jaramillo, J.; Gomperts, R.; Stratmann, R. E.; Yazyev, O.; Austin, A. J.; Cammi, R.; Pomelli, C.; Ochterski, J. W.; Martin, R. L.; Morokuma, K.; Zakrzewski, V. G.; Voth, G. A.; Salvador, P.; Dannenberg, J. J.; Dapprich, S.; Daniels, A. D.; Farkas, O.; Foresman, J. B.; Ortiz, J. V.; Cioslowski, J.; Fox, D. J. *Gaussian 09*, revision A.02; Gaussian, Inc.: Wallingford, CT, 2010.

(69) Ren, P.; Ponder, J. W. *J. Phys. Chem. B* **2003**, *107*, 5933−5947.

(70) Ren, P.; Ponder, J. W. *J. Comput. Chem.* **2002**, *23*, 1497−1506.

(71) Stone, A. J. *J. Chem. Theory Comput.* **2005**, *1*, 1128−1132.

(72) Ren, P.; Wu, C.; Ponder, J. W. *J. Chem. Theory Comput.* **2011**, *7*, 3143−3161.

(73) Schmidt, M. W.; Baldridge, K. K.; Boatz, J. A.; Elbert, S. T.; Gordon, M. S.; Jensen, J. H.; Koseki, S.; Matsunaga, N.; Nguyen, K. A.; Su, S.; Windus, T. L.; Dupuis, M.; John, A.; Montgomery, J. A., Jr. *J. Comput. Chem.* **1993**, *14*, 1347−1363.

(74) Andzelm, J.; Wimmer, E. *J. Chem. Phys.* **1992**, *96*, 1280−1303.

(75) Godbout, N.; Andzelm, J. *DGauss*, Version 2.0, 2.1, 2.3, 4.0; Computational Chemistry List, Ltd.: Columbus, OH, 1999. The file that contains the A1, A2, and P1 auxiliary basis sets can be obtained from the CCL WWW site at http://www.ccl.net/cca/data/basis-sets/DGauss/basis.v3.html (accessed 2006 and 2011).

(76) Ponder, J. *TINKER, Software Tools for Molecular Design*, version 5.0; Washington University: St. Louis, MO, 2004. The most updated version for the TINKER program can be obtained from J. W. Ponder's WWW site at http://dasher.wustl.edu/tinker accessed 2011.

(77) Darden, T. A.; York, D.; Pedersen, L. G. *J. Chem. Phys.* **1993**, *98*, 10089−10092.

(78) Essmann, U.; Perera, L.; Berkowitz, M.; Darden, T. A.; Lee, H.; Pedersen, L. G. *J. Chem. Phys.* **1995**, *103*, 8577−8593.

(79) Sagui, C.; Pedersen, L. G.; Darden, T. A. *J. Chem. Phys.* **2004**, *120*, 73−87.

(80) Berendsen, H. J. C.; Postma, J. P. M.; van Gunsteren, W. F.; Di Nola, A.; Haak, J. R. *J. Chem. Phys.* **1984**, *81*, 3684−3690.

(81) Hu, X.; Jin, Y.; Zeng, X.; Hu, H.; Yang, W. *Phys. Chem. Chem. Phys.* **2012**, *14*, 7700−7709.

(82) Piquemal, J.-P.; Perera, L.; Cisneros, G. A.; Ren, P.; Pedersen, L. G.; Darden, T. A. *J. Chem. Phys.* **2006**, *125*, 054511.

(83) Soper, A. *Chem. Phys.* **2000**, *258*, 121−137.